Single- and Multi-layer Electroplated Microaccelerometers

Yoshihiro Konaka and Mark G. Allen (*)
Yokohama Research & Development Center, Murata Mfg. Co., Ltd.,
1-18-1 Hakusan, Midori, Yokohama 226, Japan

(*) School of Electrical and Computer Engineering
Georgia Institute of Technology, Atlanta, GA 300332-0250

Abstract

Electroplating techniques have been used to fabricate both single- and multi-layer, differential output acceleration sensors. The accelerometers detect accelerations normal to the substrate by a capacitance change between electrodes. Accelerometer beam shapes were determined using finite element (FEM) simulation, and took into account the potential for residual stress in the beams. These devices have been realized using standard ultraviolet lithography and photosensitive polyimide (PSPI) resist, electroplating, and sacrificial etch processes. Electroplated nickel was employed as a structural material (beams, proof mass, anchors and electrodes) and an evaporated copper was used both for the electroplating seed layer and as a sacrificial layer. The sensors were made on top of polyimide-coated silicon to reduce stray capacitance. The maximum capacitance change of the single- and multi-layer accelerometer (four 2 mm length beams, a 2 mm x 2 mm proof mass, and 2 micron gaps) were 0.90 and 1.77 pF per g, respectively. The sensitivity of the differential accelerometer was 1.85 V/g (1 g = 9.8 m / s^2) after hybrid packaging with an integrated diode-quad bridge circuit.

Introduction

Micromachined accelerometers are well-suited to many applications, such as airbag system and anti-lock brake systems for automobiles, and motion control for robotics. Such accelerometers have been realized using a variety of micromachining techniques, such as anisotropic etching of bulk silicon [1, 2], reactive ion etching of polysilicon, and the LIGA process [3, 4]. The use of conventional ultraviolet lithography coupled with electroplating of surface micromachined mechanical structures offers many advantages, even when compared with these well-established techniques. Surface micromachining allows realization of mechanical structures without the necessity of etching the substrate itself. The use of electroplated metal for structural elements allows fabrication to take place directly onto already-fabricated CMOS circuitry (e.g., from external foundries), since the lithography and electroplating processes are inherently low temperature. In addition, relatively large thicknesses (e.g., of proof masses) can be achieved using electroplated films in contrast with chemical vapor deposited (CVD) films. Finally, the use of conventional lithography allows the use of low cost optical masks and processes and does not require any special protection for the circuit against synchrotron radiation which might be required from a LIGA process.

Fabrication processes using standard ultraviolet (UV) lithography, UV-sensitive resists such as photosensitive polyimide (PSPI), and electroplating, are well-established [5,6]. The accelerometers described in this paper have been fabricated using these techniques. As mentioned above, the use of these processes means that the accelerometer can be fabricated on the substrates containing CMOS circuits without damage because the process has no high temperature steps. This important attribute decouples sensor fabrication from CMOS fabrication. Due to this decoupling, very low cost development and/or prototyping of fully integrated micromachined devices is possible. For example, an integrated circuit can be designed in-house, and the design sent to a foundry for fabrication. Upon receipt of the fabricated chips or wafers, the designer can complete the processing in-house without the necessity of establishing a CMOS processing line. The subsequent micromachining process is simple and can be carried out using commercially available materials and common clean room equipment far less expensive than a full CMOS line. Thus, access to integrated micromechanical structures potetially at very low cost is enabled.

In this paper, the design of the microaccelerometer, the results of FEM simulation, details of the fabrication process, the capacitance change of the sensing elements

0-7803-2985-6/96 $5.00 © 1996 IEEE

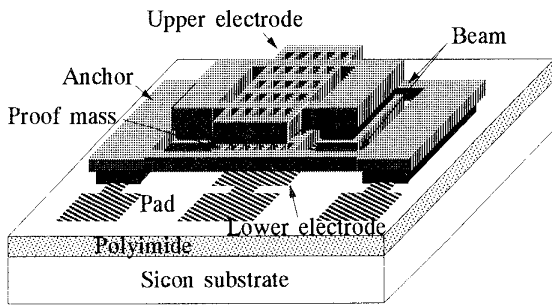

Fig. 1 Schematic of the multi-layer microaccelromater

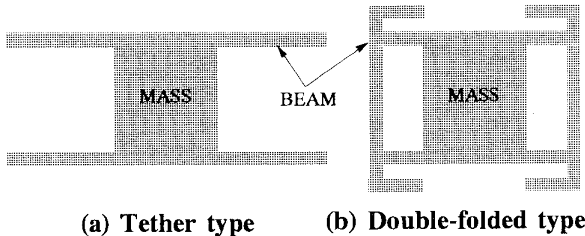

Fig. 2 Shapes of the beam

as a function of acceleration, and the sensitivity and frequency response of the accelerometer system after signal processing through a capacitance-voltage circuit are presented.

Structure and Operation

Two types of microaccelerometer, a single capacitance type and a differential capacitance type, shown in Figure 1, were investigated. The single capacitance type accelerometer consists of a proof mass which also acts as a moving electrode; beams; anchors; and a lower fixed electrode. The proof mass has a number of holes in order to easily etch the underlying sacrificial layer during fabrication. The sensor is made on top of polyimide-coated silicon to reduce stray capacitance between the silicon substrate and anchors. In normal operation, a capacitance is formed between the proof mass and the lower electrode. As the sensors are subjected to accelerations normal to the substrate, the proof mass moves due to the resultant inertial force. This displacement is detected by a capacitance change between the moving electrode and the lower electrode. In the differential capacitance type accelerometer, an additional fixed upper electrode is located over the proof mass, resulting in a multi-layer, differential capacitance device. Although the fabrication process of the differential capacitance accelerometer is more complex than that of the single capacitance accelerometer, the

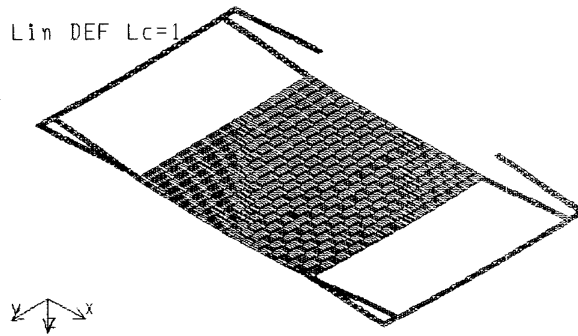

Fig. 3 The typical 3-D simulated result of the tether type beam accelerometer

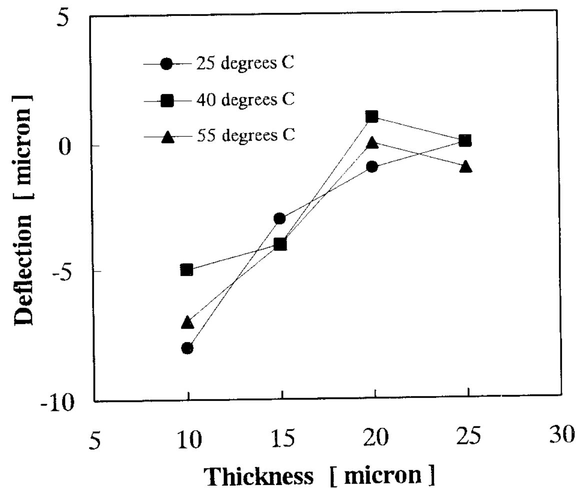

Fig. 4 Out-of-plane deflection of the catilever beams

differential capacitance accelerometer has a larger capacitance change per unit acceleration. In addition, problems such as offset are reduced, and the accelerometer can be more easily employed in closed loop operation.

The beam shapes and the dimensions of the sensor were calculated using 3-D finite element (FEM) simulation (COSMOS/M). Two types of beam, a tether type and a double-folded type (shown in Figure 2), were simulated. The typical simulated result is shown in Figure 3. As a result, the stiffness of the beam varies with temperature because the thermal expansion coefficient of the electroplated nickel is approximately five times as large as that of the silicon wafer. Double-folded type beams are less sensitive to temperature due to their ability to absorb the stress generated by thermal expansion. In addition, the double-folded type beam can achieve a higher acceleration sensitivity per unit area due to the ability to fold a longer beam in the same chip area.

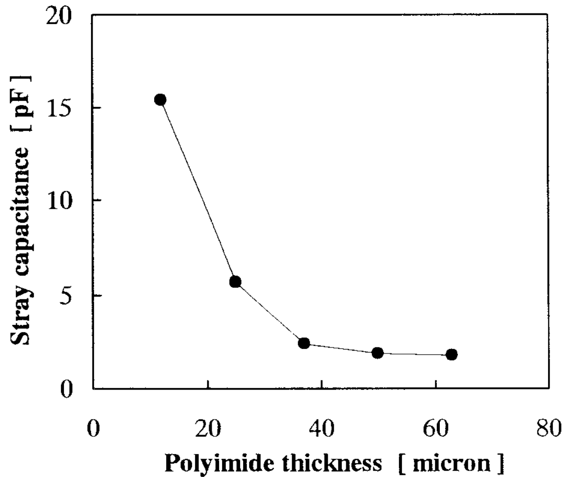

Fig. 5 Stray capacitance vs polyimide thickness

The accelerometer beams should be as free of residual stress as possible since the properties of the accelerometer can depend on the details of the residual stress of the electroplated beam. In particular, stress eccentricity can cause out-of-plane warpage of the structure. In order to assess this effect, a nickel cantilever beam 800 microns in length was fabricated to various thicknesses (10-25 microns) using the electroplating techniques described below and various plating bath temperatures (25, 40, 55 degrees C). Out-of-plane deflections of the beams were measured with a microscope. The deflection as a function of the bath temperature and the beam thickness is shown Figure 4. As expected, increasing thickness decreases the out-of-plane beam deflection. Over the ranges and baths studied, variation of bath temperature and current density have less effect. Satisfactory accelerometers could be fabricated using a bath temperature of 25 degrees C and beam thickness of 20 microns.

As a diode-quad bridge circuit is employed to transfer capacitance output to voltage output, the output voltage Vdc of the accelerometer is expressed as

$$Vdc = A \cdot (C_2 - C_1) / (C_2 + C_1 + C_s)$$

where A is a constant of proportionality, C_1 and C_2 are the capacitance outputs, and Cs is the stray capacitance. To maximize sensitivity, it is desirable to keep Cs as small as possible. The stray capacitance between the anchors (4 anchors, 1 mm x 1 mm) and lower electrode (1 mm x 1 mm) through the silicon substrate is decreased by coating the silicon with polyimide (DuPont PI-2611). Figure 5 shows the stray capacitance versus the thickness of the polyimide. For typical accelerometer geometries, when the polyimide thickness exceeds 40 microns, the stray capacitance is less than 2.5 pF, which has a sufficiently small effect on the output Vdc. As a result, silicon coated with 50 microns polyimide was employed as a substrate.

Fabrication

A brief fabrication procedure of the differential capacitance accelerometer is given in Figure 6, and detailed below. The process starts with oxidized (300 nm) 3-inch silicon wafers as a substrate. A polyimide

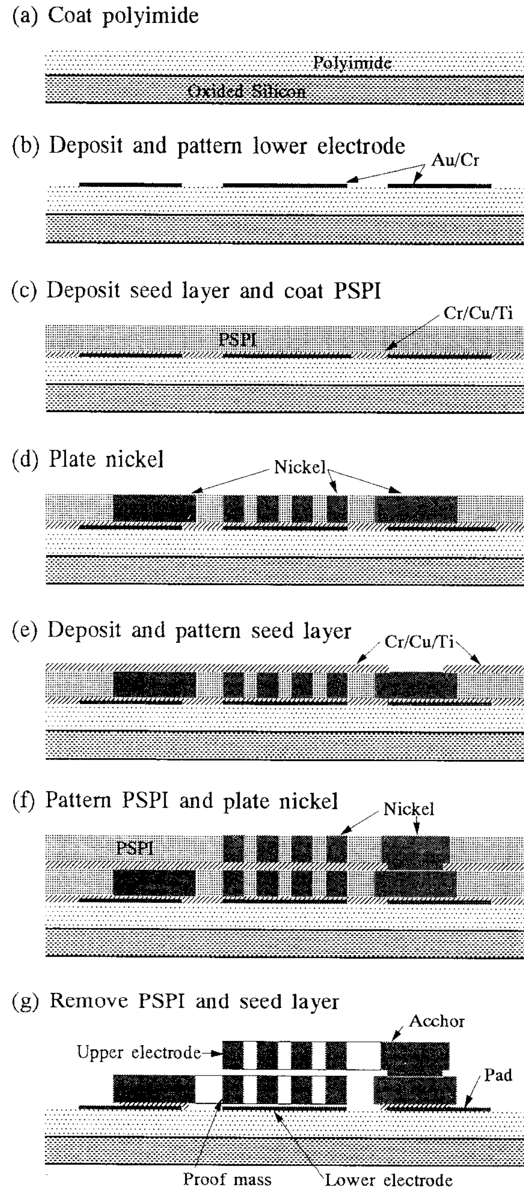

Fig. 6 Schematic of the fabrication procedure of the differential capacitance accelerometer

Table 1 Composition of the nickel electroplating solution

Component	Quantity g / l
$NiSO_4 \cdot 6H_2O$	200
$NiCl_2 \cdot 6H_2O$	5
H_3BO_3	25
Saccharin	3

(DuPont PI-2611) is spun onto the wafer to reduce stray capacitance. Five coats are used to obtain a thick polyimide film. Each coat is cast at 3000 rpm, and soft baked for 10 minutes at 120 degrees C prior to the application of the next coat. After the deposition of all coats, the polyimide is cured at 350 degrees C for 1 hour in nitrogen, yielding an after-cure thickness of 50 microns. An adhesion layer of 50 nm chromium followed by 300 nm gold layer is evaporated using an electron-beam (E-beam) evaporator and patterned for use as the lower electrode. A seed layer consisting of 50 nm titanium / 2 microns copper / 100 nm chromium (Ti/Cu/Cr) is deposited using an E-beam evaporator. A copper layer is used both for the electroplating seed layer and as a sacrificial layer. A photo-sensitive polyimide (PSPI), Ciba-Geigy Probimide 349, is then spin-cast at 200 rpm for 30 seconds on the substrate, and soft bake for 30 minutes at 110 degrees C, followed by contact imaging using a standard G-line (436 nm) mask aligner to build electroplating molds for the proof mass and the beams. The patterns in the PSPI are then developed using Ciba-Geigy QZ 3301 developer and rinsed using QZ 3312 rinse. The thickness of the mold is approximately 20 microns and the uniformity is ± 2 %. Nickel is used as a structural material and is deposited using standard electroplating techniques. The nickel plating solution composition is shown in Table 1, and the electroplating is carried out at room temperature using a current density of approximately 5 mA / cm^2. To build the upper electrode, a second Ti/Cu/Cr layer is deposited using the E-beam evaporator. This Ti/Cu/Cr layer is then etched out in the anchor areas so that the anchors are directly plated on the top of the first electroplated nickel. A second PSPI layer is spin-cast and imaged using similar conditions as the first layer, and the second nickel layer is electroplated. When the electroplating is complete, the PSPI molds are etched using 20% CF_4/O_2 plasma. The copper sacrificial layer is then selectively etched using a wet etch to release the structure. These etches typically took 0.5 hours and two hours, respectively. In the case of the single capacitance accelerometer, the second electroplating process (Ti/Cu/Cr deposition, PSPI deposition and patterning, and nickel electroplating) is omitted.

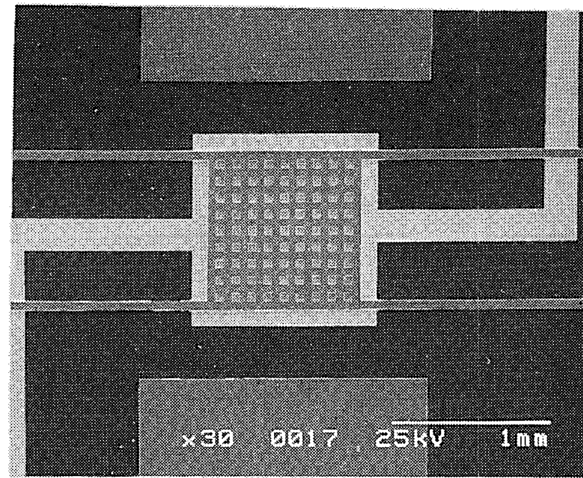

(a)

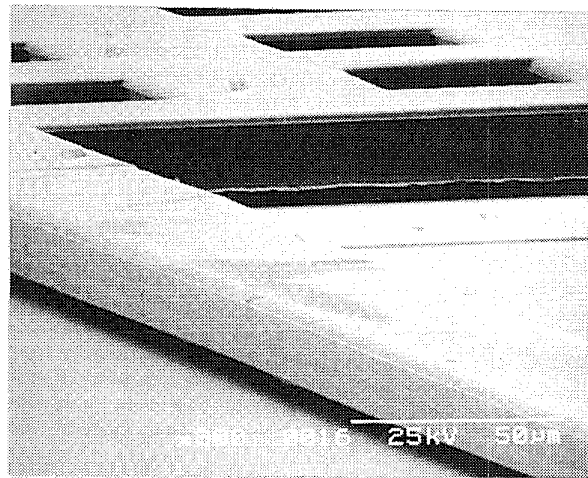

(b)

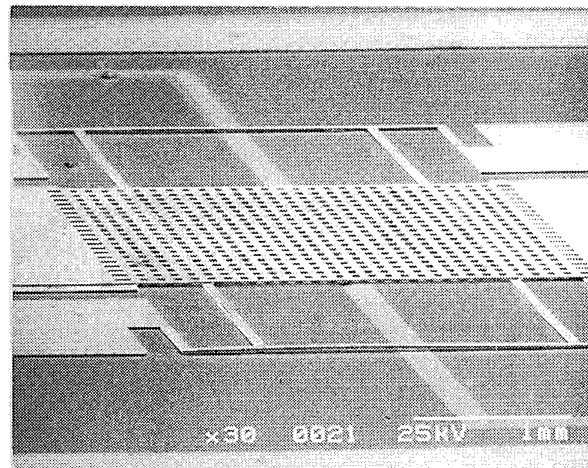

(c)

Fig 7 Scanning electron micrograph of (a), (b) a top view of the single capacitance accelerometer, (c) an angular view of the differential capacitance accelerometer

Table 2 Dimensions of the Measured Accelerometers

	Capacitance	Beam Shape	Beam Length mm	Beam Width micron	Thickness micron	Proof Mass mm x mm	Gap micron
Type A	Differential	Tether	2.0	50	20	2 x 2	2
Type B	Single	Tether	2.0	50	20	2 x 2	2
Type C	Differential	Double-Folded	2.0	50	20	2 x 2	2
Type D	Single	Double-Folded	2.0	50	20	2 x 2	2

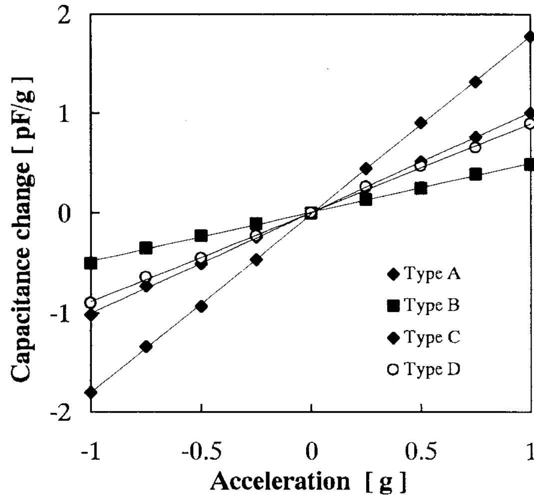

Fig. 8 The capacitance change vs input acceleration

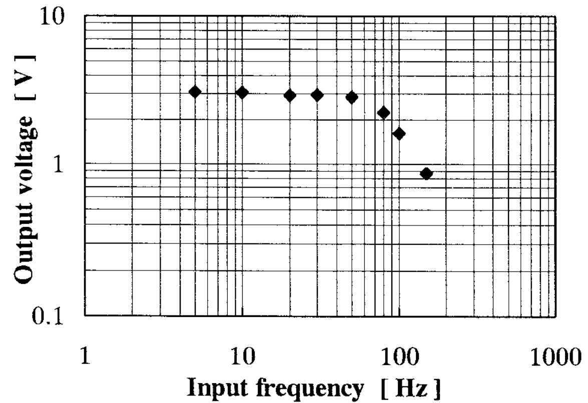

Fig. 9 Frequency response of the differential accelerometer at 2 g

Scanning electron micrographs of the fabricated accelerometers are shown in Figure 7. Figure 7(a) is a top view of the single capacitance accelerometer with the tether beams, while Figure 7(b) is an angular view. The beam length is 2 mm, the proof mass size is 1 mm x 1 mm, the thickness is 20 microns, and the gap between electrodes is 2 microns. An angular view of the differential capacitance accelerometer is shown in Figure 7(c). The proof mass locates the center between the upper and the lower electrodes.

Accelerometer Characteristics

The dimensions of the characterized accelerometers are shown in Table 2. The measured sensors include both single and differential capacitance devices, each of which have tether type and double-folded type beams. Figure 8 shows the capacitance change with input (DC) acceleration ($\pm$1 g), obtained by rotation of the sensor. In all types of the accelerometers, the capacitance changes are in proportion to the acceleration within this acceleration range. In addition, the double-folded type accelerometer shows a higher capacitance change than the tether type. The maximum capacitance change is 1.77 pF/g (as expected, for the differential capacitance sensor and double-folded beam geometry). The sensitivity and frequency response of the accelerometer system after signal processing through a capacitance-voltage circuit is measured. A integrated diode-quad bridge circuit including a operational amplitude circuit is employed. Using this integrated circuit, the sensitivity is 1.85 V/g (the capacitance change; 0.82 pF/g) at 20 Hz. Figure 9 shows the measured frequency response. The cut off frequency is 50 Hz at $\pm$2 g.

Conclusions

Electroplating techniques have been used to fabricate both single- and multi-layer, differential output acceleration sensors. Beam shapes were determined from FEM analyses and took into account potential residual stresses in the beams. These devices were realized using standard PSPI-based ultraviolet lithography, electroplating, and sacrificial etch processes. The maximum capacitance changes for the single- and multi-layer accelerometers (four 2 mm length beams, a 2 mm x 2 mm proof mass, and 2 micron gaps) were 0.90 and 1.77 pF/g, respectively. The sensitivity of the differential accelerometer was 1.85 V/g after hybrid

packaging with an integrated diode-quad bridge circuit. Although it was not demonstrated in this work, it is straightforward to fabricate an integrated microaccelerometer directly on foundry-fabricated CMOS circuits without damage because the process completely decouples sensor fabrication from CMOS fabrication.

Acknowledgment

This work was supported in part by Murata. Microfabrication discussed in this work was carried out in the Georgia Tech Microelectronics Research Center (MiRC). The authors wish to thank the MiRC staff as well as J. B. Lee and W. P. Taylor of Georgia Tech. The authors would also like to thank K. Ohwada, Y. Negoro, H. Kawai of Murata Mfg. Co., Ltd., Yokohama R & D Center for valuable technical discussions during the course of this work.

References

[1] N. Ura and M. Esashi, "Differential Capacitance Silicon Accelerometer," in Proc.10th Sensor Symposium, 1991. pp.41-44

[2] A. Koide, K. Sato, S. Suzuki, and M. Miki, "A Multistep Anisotropic Etching Process for Producing 3-D Silicon Accelerometers," in Proc. 11th Sensor and Symposium, 1992. pp. 23-26.

[3] C. Burnbaum, J. Mohr, and P.Bley, "Fabrication of capacitive acceleration sensors by the Liga technique," Sensors and Actuators, vol. 25-27, pp. 559-563, 1991.

[4] J. Mohr, P.Bley, C. Burnbaum, W. Menz, and U.Wallrabe, "Fabrication of microsensor and microactuator elements by the Liga-process," in Proc. 6th Int. Conf. Solid-State Sensor and Actuators (San Francisco, CA), 1991, pp.607-609.

[5] A. B. Frazier and M. G. Allen, "Metallic Microstructures Fabricated Using Photosensitive Polyimide Electroplating Molds," Journal of Micro Electro Mechanical Systems, vol. 2, No. 2, 1993.

[6] M. W. Putty and, K. Najafi, "A Micromachined Vibrating Ring Gyroscope," in Proc. Solid-State Sensor and Actuators (Hilton Head, SC), 1994, pp.213-220.